

Supporting Information

Integrated Battery-Capacitor Storage System: Polyaniline interwoven Co-ZIF derived hollow NiCo-LDH with high electrochemical properties for hybrid supercapacitors

Hao Guo*, Jiaying Tian, MingYue Wang, Yuan Chen, Ning Wu, Liping Peng,
Yinsheng Liu, Xijia Xu, Wu Yang*

Key Laboratory of Eco-functional Polymer Materials of the Ministry of Education; Key Lab of Bioelectrochemistry and Environmental Analysis of Gansu Province; College of Chemistry and Chemical Engineering, Northwest Normal University, Gansu International Scientific and Technological Cooperation Base of Water-Retention Chemical Functional Materials, Lanzhou 730070, PR China

Chemicals:

Co(NO₃)₂·6H₂O, Ni(NO₃)₂·6H₂O (Zhiyuan Chemical Co. Ltd., Tianjin, China), 2-methylimidazole (Hmim, Aladdin Industrial Co. Shanghai, China), aniline (Ani, Tianjin kaitong chemical reagent Co. Ltd., Tianjin, China), hydrochloric acid (HCl, Sionpharm Chemical Reagent Co. Ltd), thioacetamide (TAA, Aladdin Industrial Co., Tianjin, China), ammonium persulfate (APS, Aladdin Industrial Co., Tianjin, China), ethanol absolute (Damao Chemcial Reagent Factory, Tianjin, China) and activated carbon (AC, Shanghai Sino Tech Investment Management Co., China). All the used reagents were analytically pure and used without further purification. All deionized water (DI) used in the experiment was prepared in the laboratory with a secondary distillation tube.

* Corresponding authors. Email:xbsfda123@126.com (W Yang) and haoguo12@126.com (H Guo).

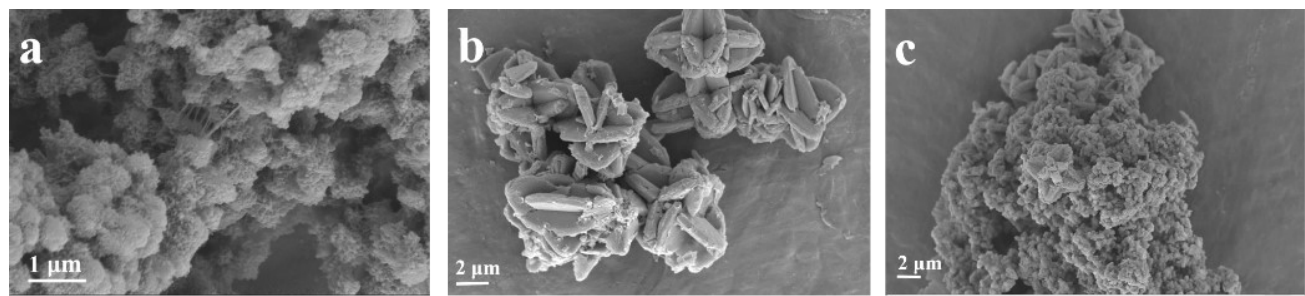


Fig. S1. SEM images of (a) PANI, (b) NiCo-LDH, (c) NiCo-LDH@PANI.

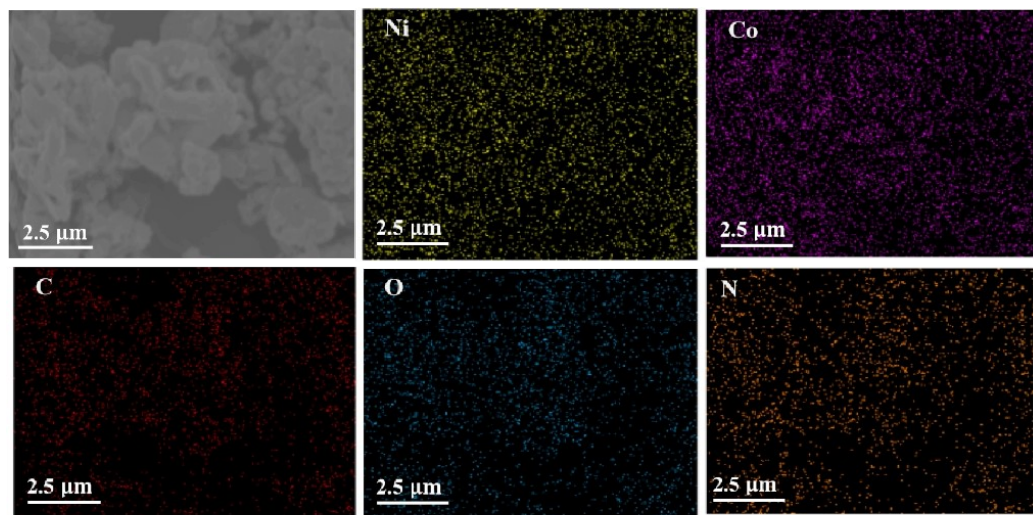


Fig. S2. EDS elemental mapping of NiCo-LDH@PANI.

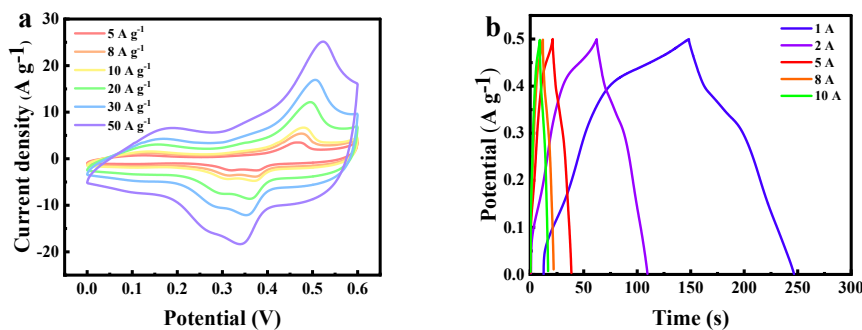


Fig. S3. (a) CV and (b) GCD curves of Co-ZIF-2@PANI.

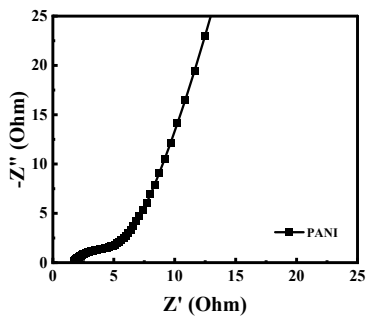


Fig. S4. Nyquist plot of PANI.

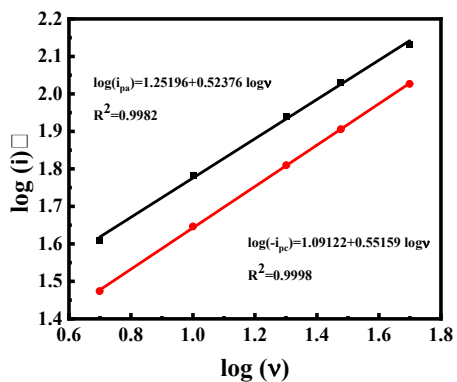


Fig. S5. Linear relationship between $\log i$ and $\log v$ of NiCO-LDH@PANI

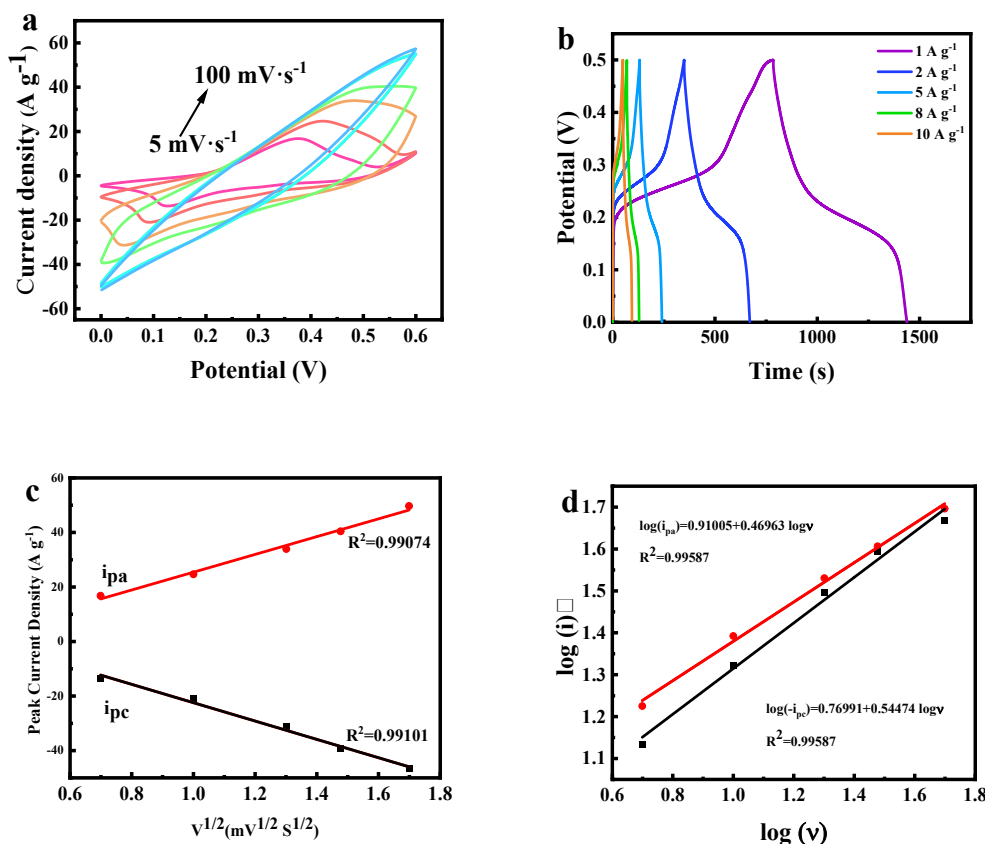


Fig. S6. (a) CV curves at different scan rates and (b) GCD curves at different current densities of NiCo-LDH, (c) the relationship between the peak current (i_p) and the power of one-half of the scan rate ($v^{1/2}$) and (d) linear relationship between $\log(i)$ and $\log(v)$.

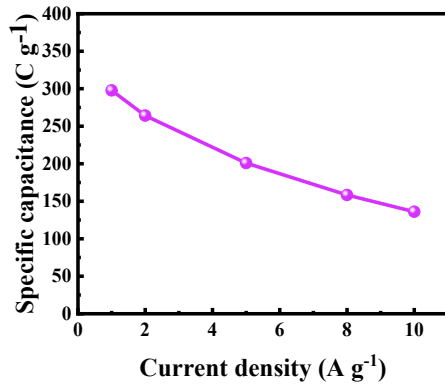


Fig. S7. Specific capacitances at different current densities of the BSH device.

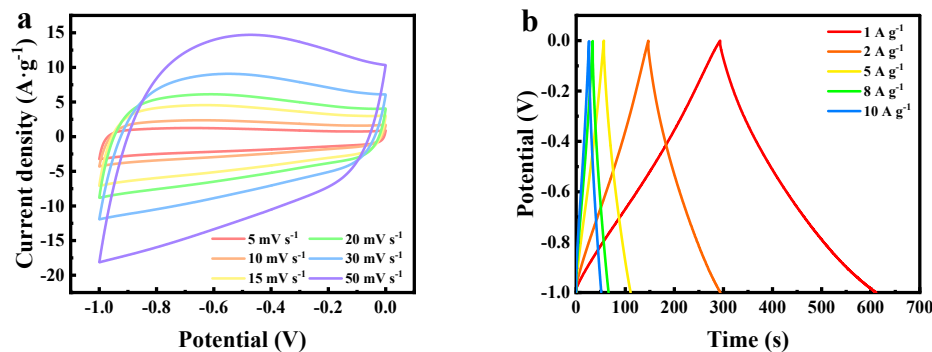


Fig. S8 (a) CV curves of AC at different scan rates, (b) GCD curves of AC at different current